Cell Stress and Chaperones (2022) 27:673–684
https://doi.org/10.1007/s12192-022-01304-x

ORIGINAL ARTICLE

# PBX1 attenuates $H_2O_2$-induced oxidant stress in human trabecular meshwork cells via promoting NANOG-mediated PI3K/AKT signaling pathway

**Liang Wang[1] · Ying Tian[1] · Yan Cao[1] · Qiang Ma[1] · Shuai Zhao[1]**

Received: 18 April 2022 / Accepted: 4 October 2022 / Published online: 18 October 2022


**Abstract**
Oxidative stress–induced excessive extracellular matrix (ECM) deposition in trabecular meshwork (TM) tissue is considered the major pathological procedure of glaucoma. This study aimed to explore the role and regulatory mechanism of pre-B-cell leukemia transcription factor 1 (PBX1) in $H_2O_2$-induced human trabecular meshwork cells (HTMCs). Expressions of PBX1, NANOG, ECM, and pathway-related factors were detected by qRT-PCR and western blot. Cell viability and apoptosis of HTMCs were measured using CCK-8 and flow cytometry assays. Reactive oxygen species (ROS), superoxide dismutase (SOD), and L-glutathione (GSH) levels were detected to evaluate oxidative stress. Through luciferase reporter assay, the association between PBX1 and NANOG was verified. Results presented that PBX1 was significantly upregulated in $H_2O_2$-induced HTMCs. Functionally, PBX1 and NANOG promoted cell viability, inhibited cell apoptosis and ECM deposition, suppressed ROS accumulation, and enhanced the productions of SOD and GSH in $H_2O_2$-stimulated HTMCs, while PBX1 inhibition showed the opposite effects. In addition, PBX1 promoted the transcription of NANOG by upregulating the promoter activity of NANOG which activated the PI3K-AKT signaling pathway. What's more, the inhibitions of PI3K-AKT signaling pathway or NANOG reversed the protective effect of PBX1 on $H_2O_2$-stimulated HTMCs. In summary, our study firstly revealed that PBX1 attenuated the oxidative damage in HTMCs via regulating NANOG-mediated PI3K/AKT signaling, suggesting that PBX1 might be a potential treatment target for glaucoma patients.

**Keywords** Glaucoma · PBX1 · NANOG · Trabecular meshwork · Oxidative stress · PI3K/AKT

## Introduction

Glaucoma is the second leading cause of blindness in the world, characterized by progressive and irreversible vision loss (He et al. 2018). Primary open-angle glaucoma (POAG) is the most common type of glaucoma whose major risk factor is regarded as elevated intraocular pressure (IOP) (Bertaud et al. 2019). Aqueous humor (AH) is responsible for maintaining intraocular pressure (Carreon et al. 2017). Trabecular meshwork (TM) dysfunction could cause AH drainage dysfunction and lead to elevated IOP (Braunger et al. 2015). Human TM cell apoptosis and excessive deposition of extracellular matrix (ECM) components in TM tissue are regarded as the main pathological manifestations of OAG and induce physiological alteration in the outflow pathway of TM (Agarwal and Agarwal 2018). Besides, oxidative stress is also proven to participate in the pathogenesis of glaucoma (McMonnies 2018). Abnormal oxidative DNA damage was found to be aggravating in the TM during glaucoma progression (Saccà et al. 2016). It has been reported that $H_2O_2$-caused oxidative stress could lead to the loss of TM cells and elevate resistance to AH outflow in vivo (Izzotti et al. 2003). Hence, the inhibition on oxidative stress–induced TM damage may be an effective strategy for the treatment of glaucoma (McMonnies 2018).

PBX1 (pre-B-cell leukemia transcription factor 1) is a stem cell reprogramming factor, and plays an important role in the development of the pancreas, spleen, kidney, urogenital tract, and skeleton (Ferraz-de-Souza et al. 2009; Schnabel et al. 2003; Teoh et al. 2010). It also plays an essential role in corneal morphogenesis. The loss of PBX1 leads to corneal dystrophy and clouding in newborns. Furthermore, PBX1

✉ Shuai Zhao
hangsomezhao@163.com

[1] Department of Ophthalmology, Xi'an No. 1 Hospital, No. 30 Powder Lane South Street, Xi'an 710002, China

deletion caused the thickening of cornea epithelium, disorganization of stromal collagen matrix, and loss of corneal barrier function (Murphy et al. 2010). From Gene Expression Omnibus (GEO) database, PBX1 was identified to be significantly upregulated in glaucoma samples compared with the normal group. And PBX1 was also increased in the tissue of an acute IOP elevation rat model (Wang et al. 2017). In addition, it was reported that PBX1 protected dopaminergic neurons against oxidative stress by inducing Nfe2l1 (J. C. Villaescusa et al. 2016a, b). However, the specific role of PBX1 in oxidative stress–induced TM damage remains unclear.

Accumulating evidence indicated that oxidative stress depressed the PI3K-AKT signaling pathway (Wang et al. 2019; Zhuang et al. 2019) which played a neuroprotection role against ocular hypertension–induced retinal ganglion cells' (RGCs) injury (Husain et al. 2017; Li et al. 2017). Li et al. (2017) reported that lncRNA-MALAT1 suppressed RGC apoptosis in an IOP-elevated glaucoma rat model via activating the PI3K/AKT signaling pathway. Besides, PBX1 was reported to suppress cell apoptosis and promote the proliferation and reprogramming of hair follicle mesenchymal stem cells via activating the AKT signaling pathway (Jiang et al. 2019; Wang et al. 2020).

In this study, $H_2O_2$-induced human trabecular meshwork cell (HTMC) model was established as an oxidative damage model (Lv et al. 2020). Gain-of- and loss-of-function experiments were performed to explore the function of PBX1 on regulating cell viability, apoptosis, oxidative stress, and ECM metabolism in $H_2O_2$-stimulated HTMCs. Furthermore, the underlying mechanisms of PBX1 in oxidative injured progression of HTMCs were investigated.

## Materials and methods

### Cell culture and treatment

The establishment of in vitro glaucoma model in this study was based on previous research (Ammar et al. 2012). Primary human trabecular meshwork cells (HTMCs) were purchased from iCell Bioscience, Inc. (Shanghai, China), and cultured in normal DMEM medium (Gibco, Grand Island, NY, USA) containing 15% fetal bovine serum (FBS, Gibco) and 5 mL TM cell growth supplement under a condition of 5% $CO_2$ at 37 °C.

$H_2O_2$ treatment: HTMCs (passages at 3 to 5) were incubated with 0, 100, 200, 400, and 800 μM $H_2O_2$ (Sigma-Aldrich) in serum-free medium for 3 h, respectively, and then allowed to grow in fresh medium for another 21 h. An inhibitor of AKT pathways, LY294002, was purchased from Calbiochem (Darmstadt, Germany). HTMCs were exposed to LY294002 (20 μM) for 1 h before $H_2O_2$ treatment.

### Cell transfection

The overexpression vectors of human wild-type NANOG (ov-NANOG) and PBX1 (ov-PBX1), as well as the control vector (ov-NC), were purchased from Addgene (Cambridge, MA, USA). The siRNAs of PBX1 (si-PBX1), NANOG (si-NANOG), and negative control (si-NC) were constructed from Genepharma (China), whose sequences are listed in Table 1. Cell transfection was performed using a Lipofectamine 3000 kit (Invitrogen, USA) following the manufacturers' protocol.

### RNA extraction and real-time quantitative PCR

Total RNAs were isolated from HTMCs using 500 μL Trizol reagent (Invitrogen, CA, USA) along with chloroform (100 μL). Isopropanol was used to sediment and 75% ethyl alcohol was used to wash total RNA. RNA purity was measured on a NanoDrop 2000 system (Thermo Fisher, Shanghai, China) by detecting the ratio of $A_{260/280}$. An amount of 500 μg total RNA was transcribed into cDNA with the help of a PrimeScript RT Enzyme mix kit (Takara, Dalian, China). The transcription system included as follows: primer, reaction buffer, RNase inhibitor, dNTP, water, and RNA template. Subsequently, the concentration of cDNA was adjusted to 20 ng/mL which was utilized for qPCR procedure. The real-time quantitative PCR was performed by using a ChamQTM SYBR® qPCR Master Mix (Vazyme, Nanjing, China) on an Applied Biosystems 7500 Real-Time PCR System (Shanghai, China). The system of qPCR was as follows: DNA template, primer, water, and Mix solution. The relative expression of mRNA was quantified using $2^{-\Delta\Delta Ct}$ method. The primers used in the study were synthesized by Invitrogen (Shanghai, China) and their sequences are listed in Table 2.

### Cell viability assay

HTMCs were planted into 96-microwell plates at a density of $1 \times 10^4$ cells/well. After overnight incubation, cells were treated with multiple concentrations of $H_2O_2$ (0, 100, 200, 400, and 800 μM) for 3 h, respectively, then replaced with fresh culture medium and cultured for another 21 h. Cell viability of HTMCs was measured by using a Cell Counting

**Table 1** The sequences of siRNAs used in this study

| Gene names | Sequences (5'-3') |
|---|---|
| si-PBX1 | GCATCAGTGCTAATGGAGGTUTT |
| si-NC | TAGCGCATGTAACTGAGGGUTTT |
| si-NANOG | GCTTTGAAGCATCCGACTGTATT |

**Table 2** The primers used in this study

| Gene names | Sequences (5'-3') |
|---|---|
| PBX1 | F: GAGACGGAATTTCAACAAGCA<br>R: GTTTGATACCTGGGAGACTG |
| NANOG | F: ACCAGAACTGTGTTCTCTTCCACC<br>R: GGTTGCTCCAGGTTGAATTGTTCC |
| COL1A1 | F: TCTGCGACAACGGCAAGGTG<br>R: GACGCCGGTGGTTTCTTGGT |
| COL4A1 | F: TGCTTGTTGTCCAGCTGAAAT<br>R: ACAGGAGGAAAGGCAACCAC |
| Vimentin | F: GACAATGCGTCTCTGGCACGTCTT<br>R: TCCTCCGCCTCCTGCAGGTTCTT |
| fibronectin | F: AGCCGCCACGTGCCAGGATTAC<br>R: CTTA TGGGGGTGGCCGTTGTGG |
| TIMP1 | F: TCTGCAATTCCGACCTCGTC<br>R: CTGTTCCAGGGAGCCACAAA |
| MMP2 | F: TCAAGGACCGGTTCATTTGG<br>R: GGCCTCGTATACCGCATCAAT |
| MMP3 | F: GGAGGGGAAAAGGTTGAAAG<br>R: CCACGTAGCTGCTCCATAAATAG |
| GAPDH | F: AAGAAGGTGGTGAAGCAGGC<br>R: TCCACCACCCTGTTGCTGTA |

*F*, forward primer; *R*, reverse primer

Kit-8 (CCK-8, Dojindo, Kumamoto, Japan). CCK-8 reagents (10 μL) were added into each well and incubated for 2 h at 37 °C. The absorbance value was measured at 450 nm under a microplate reader (Biotek, Winooski, VT, USA). Three duplicate wells were examined for each group.

## Cell apoptosis assay

Cell apoptosis rate was measured by using an Annexin-V FITC/PI double stain assay kit (KeyGEN, Shanghai, China). HTMCs were harvested and resuspended in 500 μL buffer, then stained with 5 μL Annexin-V reagents for 20 min in the dark at room temperature. Subsequently, PI (5 μL) solution was added before being assessed on a flow cytometry (BD Biosciences, San Jose, USA). The final cell apoptosis rate was calculated using a EXP032 ADC analysis software.

## Superoxide dismutase (SOD) activity, reactive oxygen species (ROS), and glutathione (GSH) level detection

SOD activity, ROS, and GSH levels were measured by using Reactive Oxygen Species Assay Kit, Total Superoxide Dismutase Assay Kit, and Glutathione Assay Kit, respectively, according to the manufacturers' protocols (Beyotime Biotechnology, Shanghai, China). Briefly, the level of SOD was detected through spectrophotometry method by estimating the optical density of formazone formed by superoxide radicals and nitroblue tetrazolium at a wavelength of 560 nm. The treated cells were incubated with DCFH-DA (10 μM, 20 min, dark, 37 °C); the images were captured after the cells had been washed; then, ROS level was analyzed by detecting the fluorescence intensity. Based on the characteristic absorption peak of the reactants of disulfide nitrobenzene and GSH at 412 nm, the target OD value is proportional to the GSH content. The final activities of SOD and GSH were quantified in line with the standard curve using standard solution and normalized to per unit of protein contents.

## Western blotting

Western blotting assay was performed in accordance with a previous report (Lv et al. 2020). With the help of RIPA buffer (protease inhibitor contained), the total proteins of samples were extracted. A BCA analysis kit (Takara, Dalian, China) was utilized for protein quantification. For SDS-PAGE separation (10%), 20 μg protein was recruited and then transferred onto PVDF membranes. Following being incubated with 5% non-fat milk for 2 h (room temperature), the membranes were incubated with primary antibodies overnight at 4 °C. The antibodies were used as follows: anti-PBX1 (ab97994), anti-fibronectin (ab2413), anti-TIMP1 (ab211926), anti-MMP2 (ab86607), and anti-MMP3 (ab52915) were purchased from Abcam (Cambridge, MA). Anti-NANOG (#4903), anti-PI3K p100α (#4249), anti-p-AKT (Ser473, #4060), anti-AKT (#9272), anti-COL1A1 (#72,026), anti-COL4A1 (#50,273), and anti-Vimentin (#5741). All the antibodies were purchased from Cell Signaling Technology (Boston, MA, USA). Goat Anti-Rabbit (ab205718) and Goat Anti-Mouse (ab205719) IgG H&L (HRP) were purchased from Abcam (Cambridge, MA) and used to incubate the membranes for another 2 h. GAPDH (ab8245, Abcam) acted as the control. The protein bands were imaged by a LI-COR Odyssey System (LI-COR Biotechnology, USA). Finally, the gray value of protein bands was quantified by ImageJ software.

## Dual-luciferase reporter assays

A previous study indicated that the CR1 and CR2 (− 1897 ~ − 239) regions of NANOG promoter were important for PBX1 trans-activation (K. K. Chan et al. 2009a, b). Hence, in this study, the wild type (WT-NANOG) and mutant type (MUT-NANOG) of NANOG 3′UTR regions were cloned into pGL3 luciferase reporter vector (Promega, Madison, WI, USA). HTMCs were cultured in 24-well plates and co-transfected with WT-NANOG or MUT-NANOG along with ov-PBX1 or ov-NC plasmids. After 24 h, the transfected cells were treated with 200 μM $H_2O_2$ in serum-free medium for 3 h, and then allowed to grow in fresh media for approximately 21 h. Then, the relative light units (RLUs)

were measured by a Dual-Luciferase Reporter Gene Assay Kit (Beyotime Biotechnology, China).

### Data analysis

Data were expressed as mean ± standard error of mean (SEM) and analyzed by using SPSS 13.0 (IBM, Armonk, NY, USA). Student's *t*-test and one-way analysis of variance (ANOVA) followed by post hoc comparison were adopted to analyze the statistical significance of two groups or more than two groups. Statistical significance was established at $P < 0.05$. The specific $P$ values were marked in figures and supplementary tables (Tables 3 ~ 11).

## Results

### *PBX1 expression was increased in $H_2O_2$-stimulated HTMCs*

We first exposed $H_2O_2$ s to induce oxidative injury in HTMCs. As shown in Fig. 1A, the cell viability of HTMCs was obviously declined after treated with $H_2O_2$ compared with the control group, in a dose-dependent manner. Meanwhile, the expression of PBX1 was significantly increased in $H_2O_2$-stimulated HTMCs (Fig. 1B and C). In the following experiments, HTMCs stimulated with 200 μM $H_2O_2$ were utilized to establish the oxidative injury model of trabecular meshwork cells.

### *Effects of PBX1 overexpression and inhibition on the viability, apoptosis, and oxidative stress in $H_2O_2$-stimulated HTMCs*

To explore the role of PBX1 in $H_2O_2$-stimulated HTMCs, the overexpression plasmid of PBX1 (ov-PBX1) and si-PBX1 were transfected into HTMCs. The results suggested that the expression of PBX1 was significantly upregulated by ov-PBX1 and downregulated by si-PBX1 (Fig. 2A, B, C). The overexpression of PBX1 significantly inhibited the decline of viability and apoptosis elevation in HTMCs induced by $H_2O_2$ treatment, while PBX1 inhibition aggravated the loss of cell viability and promoted cell apoptosis in $H_2O_2$-treated HTMCs (Fig. 2D and E). Besides, the overexpression of PBX1 significantly increased SOD activity and GSH levels in $H_2O_2$-treated HTMCs, while the silence of PBX1 decreased the activity of SOD and the level of GSH in $H_2O_2$-treated HTMCs (Fig. 2F and H). Additionally, the overexpression of PBX1 significantly suppressed the increase of ROS production in $H_2O_2$-treated HTMCs and the silence of PBX1 presented an opposite effect (Fig. 2G).

### *Effects of PBX1 overexpression and inhibition on ECM metabolism in $H_2O_2$-stimulated HTMCs*

Next, the expressions of ECM metabolism–related genes were measured in $H_2O_2$-treated HTMCs. As shown in Fig. 3, both the mRNA and protein expressions of COL1a1, COL4a1, vimentin, fibronectin, MMP2, and MMP3 were suppressed by PBX1 overexpression, and promoted by PBX1 inhibition in $H_2O_2$-stimulated HTMCs. At the same time, TIMP1 (tissue inhibitor of matrix metalloproteinases) was upregulated by PBX1 overexpression and suppressed by PBX1 inhibition in $H_2O_2$-stimulated HTMCs (Fig. 3).

### Effects of NANOG overexpression on $H_2O_2$-stimulated HTMCs

Previous studies reported that PBX1 promoted the transcription of NANOG by upregulating promoter activity (K. K. Chan et al. 2009a, b; Jiang et al. 2019). In our study, we found that the overexpression of PBX1 significantly promoted the luciferase activity of NANOG promoter in WT-NANOG transfected group, compared with MUT-NANOG transfected group (Fig. 4A). Meanwhile, PBX1 overexpression promoted the mRNA and protein

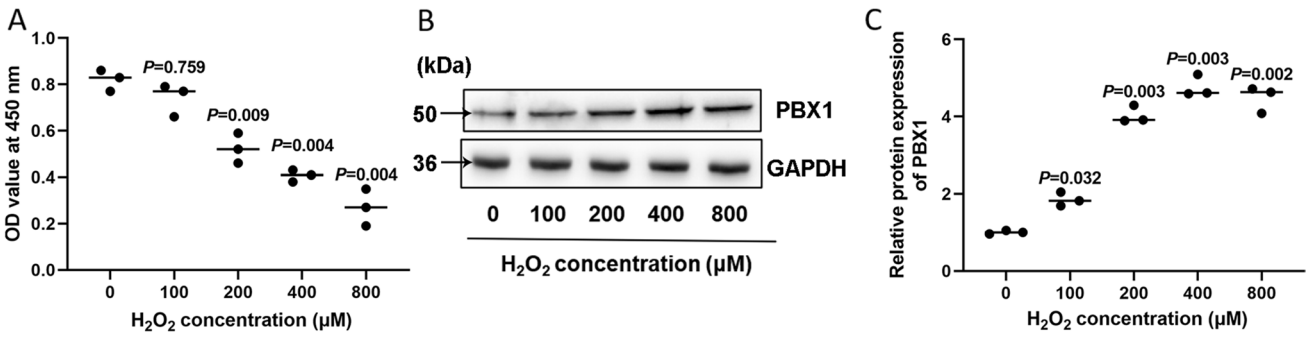


**Fig. 1** $H_2O_2$ treatment promoted PBX1 protein expression in HTMCs. Cell viability (**A**) and protein expression of PBX1 (**B** and **C**) in HTMCs were measured through CCK-8 assay kit and western blotting. HTMCs were incubated with different concentrations of $H_2O_2$ in serum-free medium for 3 h, and then allowed to grow in fresh media for approximately 21 h. Data are shown as individual spots

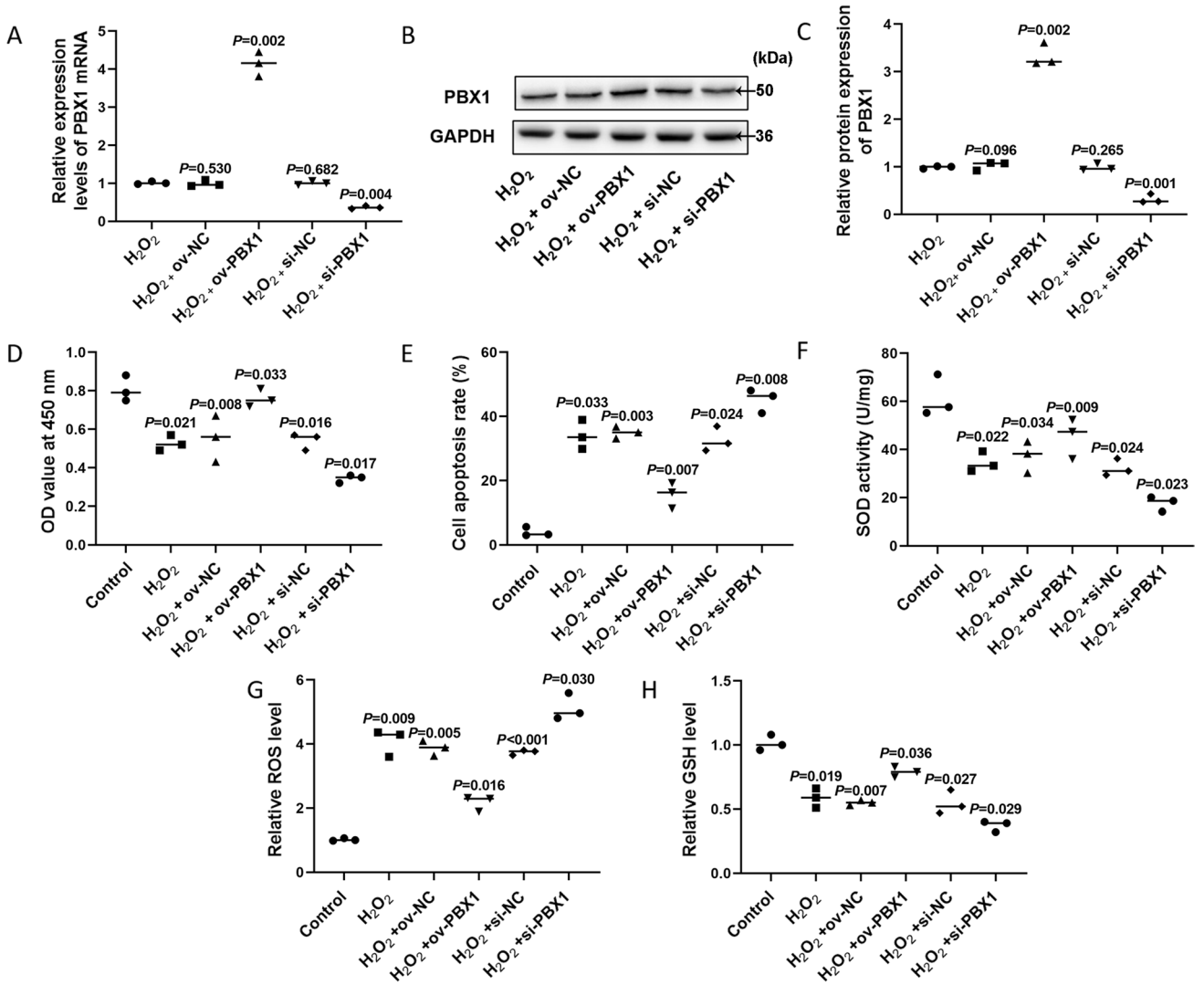


**Fig. 2** Effects of PBX1 overexpression and inhibition on the viability, apoptosis, and oxidative stress in $H_2O_2$-stimulated HTMCs (200 μM, 3 h). **A–C** Expressions of PBX1 mRNA (**A**) and protein (**B** and **C**) were measured after transfection with the overexpression plasmids of PBX1 (ov-PBX1) or siRNA of PBX1 (si-PBX1) in $H_2O_2$-stimulated HTMCs. **D–H** Cell viability (**D**), apoptosis (**E**), SOD activity (**F**), ROS (**G**), and GSH (**H**) levels were measured in $H_2O_2$-stimulated HTMCs. After transfection with ov-PBX1 or si-PBX1 for 24 h, HTMCs were stimulated with 200 μM $H_2O_2$ in serum-free medium for 3 h. Approximately post 21 h, cells were harvested for further investigation. Data are shown as individual spots

expressions of NANOG in $H_2O_2$-stimulated HTMCs (Fig. 4B and C). In addition, we found that the overexpression of NANOG significantly promoted cell viability and suppressed cell apoptosis in $H_2O_2$-stimulated HTMCs (Fig. 4D and E). Also, NANOG overexpression increased SOD activity and GSH production, and suppressed ROS production in $H_2O_2$-stimulated HTMCs (Fig. 4F, G, H). Furthermore, we explored the function of NANOG in ECM metabolism. The overexpression of NANOG significantly downregulated the mRNA and protein expression of COL1A1, vimentin, MMP2, and MMP3, and upregulated TIMP1 expression in $H_2O_2$-stimulated HTMCs (Fig. 4I–J).

## PBX1 activated the PI3K-AKT signaling pathway through promoting NANOG transcription

The expression levels of PI3K, p-AKT, and AKT in HTMCs were measured after being treated with 200 μM $H_2O_2$ for 0, 30, 60, 120, and 180 min. The results showed that after $H_2O_2$ treatment, the phosphorylation of AKT was increased at 30 min and then decreased in a time-dependent manner (Fig. 5A and B). NANOG expression was significantly inhibited by the transfection of si-NANOG. Next, we found that the overexpression of PBX1 significantly promoted the phosphorylation of AKT in $H_2O_2$-stimulated HTMCs, while

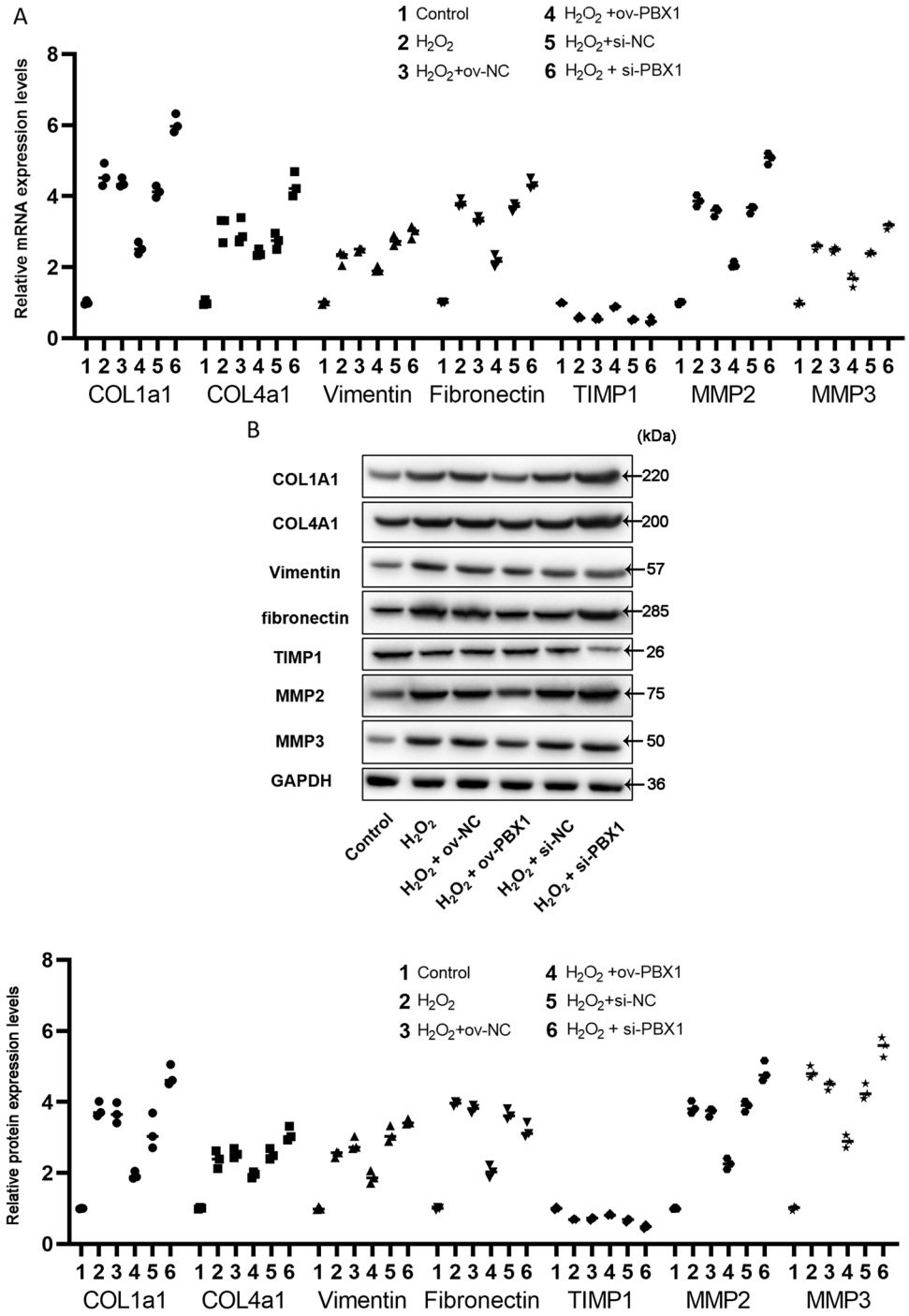


**Fig. 3** Effects of PBX1 overexpression and inhibition on ECM metabolism in $H_2O_2$-stimulated (200 μM, 3 h) HTMCs. Expressions of mRNA (**A**) and protein (**B** and **C**) levels of ECM metabolism–related genes were measured through RT-PCR and western blotting. Cell treatment was the same as described in Fig. 2. Data are shown as individual spots

the silence of NANOG weakened the promoting effect of PBX1 on p-AKT expression (Fig. 5E and F).

## The inhibition of PI3K-AKT signaling pathway or silence of NANOG abolished the protective effect of PBX1 on $H_2O_2$-stimulated HTMCs

To investigate whether PBX1 protected HTMCs from $H_2O_2$-induced oxidative injury through regulating the PI3K/AKT pathway and the expression of NANOG, LY294002 (an inhibitor of PI3K/AKT) and si-NANOG were adopted to treat HTMCs along with $H_2O_2$. The results indicated that LY dramatically depressed the activation of AKT under both normal and $H_2O_2$ treatment (Fig. 5G and H). The inhibition of PI3K-AKT signaling pathway or silence of NANOG partially abolished the effects of PBX1 overexpression on cell viability, apoptosis, SOD activity, ROS, and GSH production in $H_2O_2$-stimulated HTMCs (Fig. 6A, B, C, D, E).

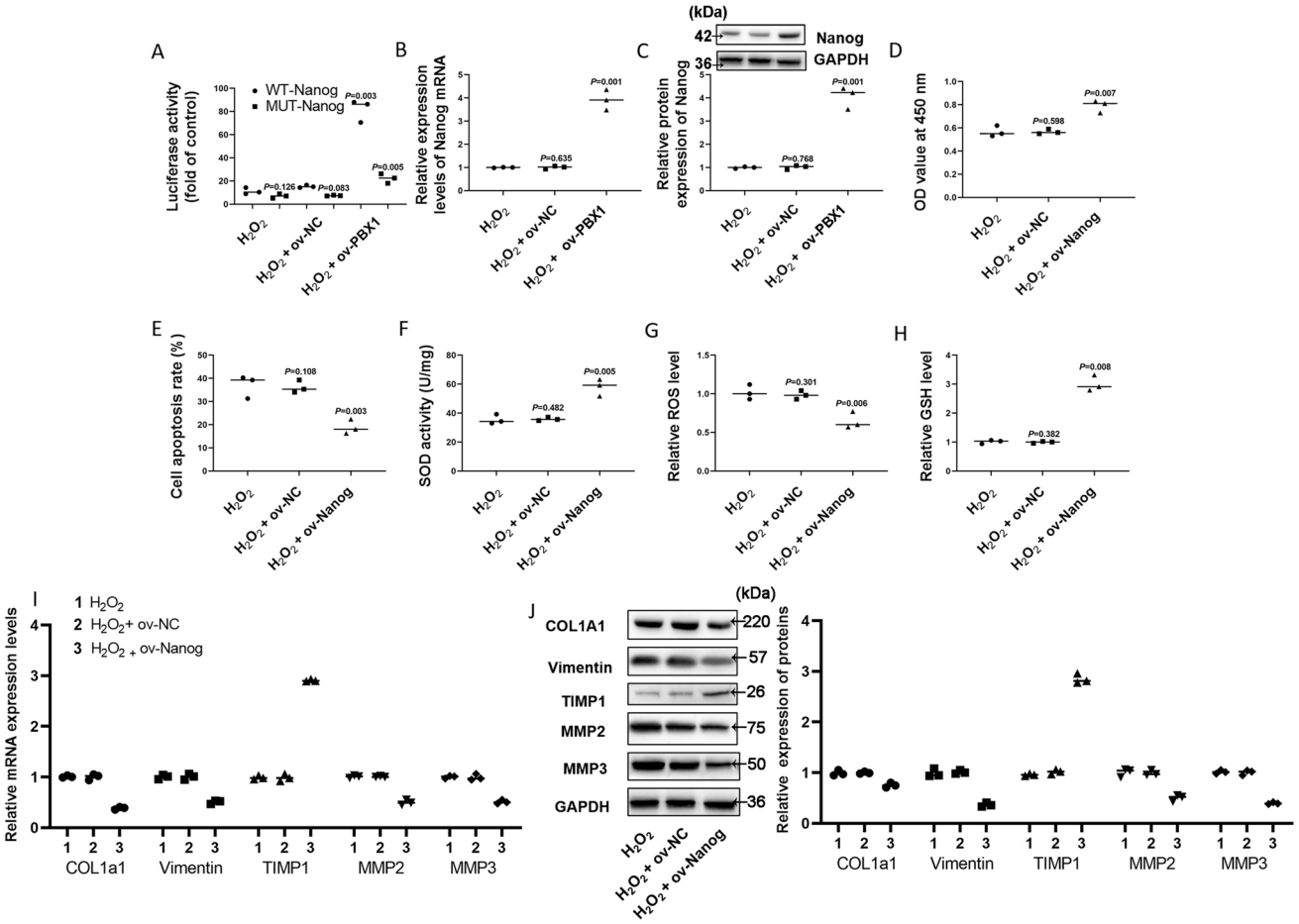


**Fig. 4** PBX1 promoted NANOG expression and the effect of NANOG overexpression on $H_2O_2$-stimulated (200 μM, 3 h) HTMCs. **A** Luciferase activity of the promoter of NANOG was measured through the dual-luciferase reporter assay. **B** and **C** The expression of NANOG mRNA (**B**) and protein (**C**) in $H_2O_2$-stimulated HTMCs. **D–H** Cell viability (**D**), apoptosis (**E**), SOD activity (**F**), ROS (**G**), and GSH (**H**) levels were measured in $H_2O_2$-stimulated HTMCs after transfection with ov-NANOG. **I** and **J** Expression levels of ECM metabolism–related genes were analyzed by RT-PCR and western blotting. Data are shown as individual spots

Meanwhile, LY294002 and si-NANOG reversed the inhibitory effects of PBX1 on COL1A1, vimentin, MMP2, and MMP3 expressions, and the promotion effect of PBX1 on TIMP1 expression (Fig. 6F, J, H).

## Discussion

Currently, increasing studies showed that antioxidants regulate intraocular pressure and protect retinal ganglion cells (RGCs) from oxidative stress injury (Pinazo-Duran et al. 2018). However, the efficiency of POAG treatment is still limited. In the present study, we successfully established an oxidative stress model in vitro and investigated the role of PBX1 in oxidative stress–injured HTMCs (Fig. 7). It was identified that PBX1 was significantly upregulated in $H_2O_2$-induced HTMCs. Meanwhile, the overexpression of PBX1 suppressed the decrease of cell viability and increase of apoptosis in $H_2O_2$-induced HTMCs, while the silence of PBX1 had the opposite effects. The results were consistent with previous studies that PBX1 had the ability to promote cell survival and growth (Jiang et al. 2019).

PBX1 is a transcriptional pioneer factor and regulates the differentiation and proliferation of stem cells (J. G. Jung et al. 2016a, b; Wu et al. 2018). Meanwhile, PBX1 exhibited an oncogenic potential in several cancer (J.-G. Jung et al. 2016a, b; Kikugawa et al. 2006; Magnani et al. 2011; Okada et al. 2015; Shiraishi et al. 2007). Since knocking out PBX1 from mouse embryos resulted in multiple organ agenesis and dysfunction, PBX1 was thought to act on nearly the apex of multiple cell fate hierarchies (Grebbin and Schulte 2017). Additionally, the knockdown of PBX1 significantly decreased the promoter activity of NANOG (Jiang et al. 2019). A previous study demonstrated that KLF4 and PBX1 directly bound to NANOG promoter and the expression of endogenous NANOG in KLF4- or PBX1-downregulated

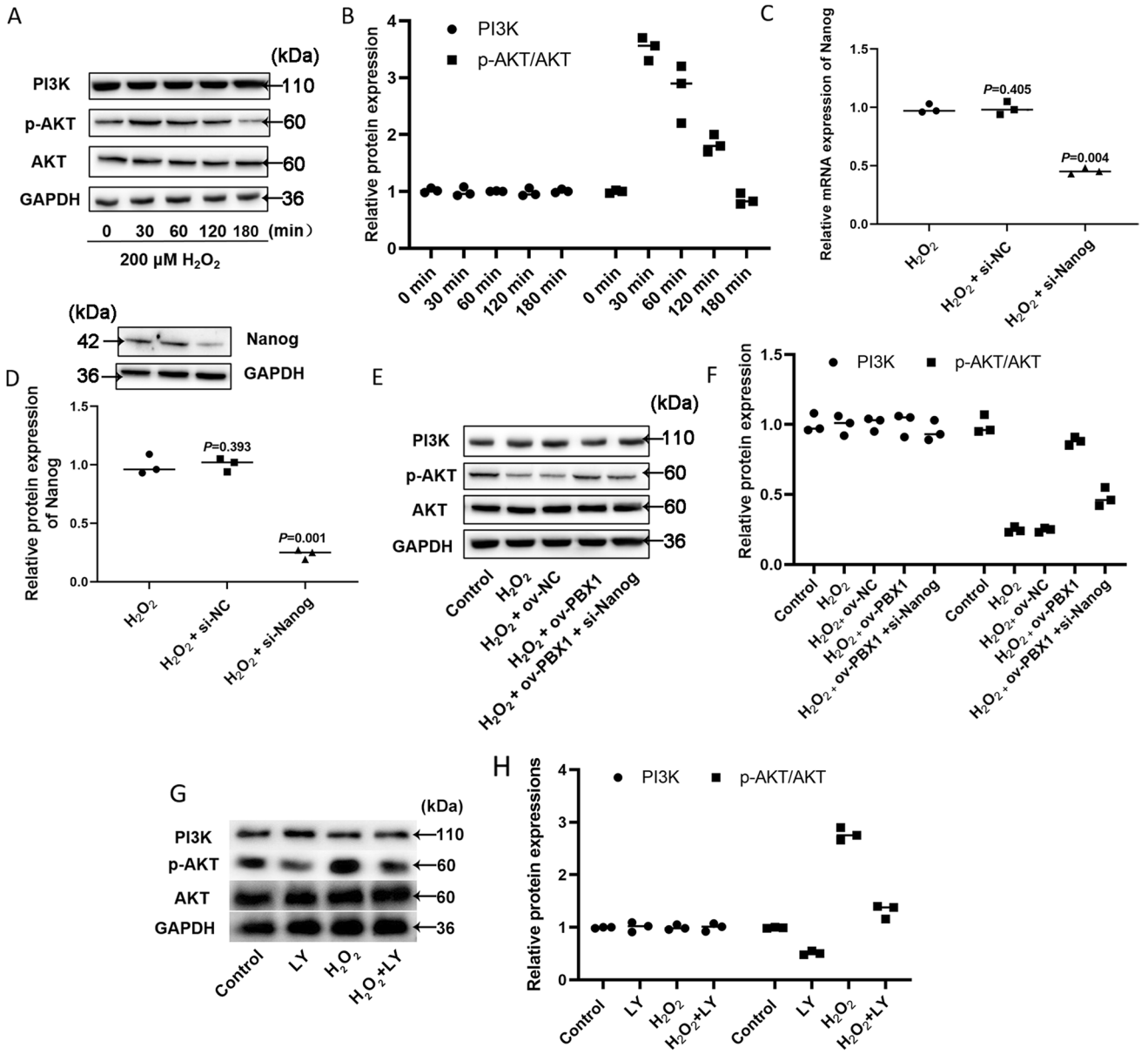


**Fig. 5** PBX1 activated the PI3K-Akt signaling pathway through promoting NANOG transcription. **A** and **B** Protein expressions of PI3K, p-AKT, and AKT were measured in HTMCs after treated by $H_2O_2$ for 0, 30, 60, 120, 180 min (200 μM). **C–D** Transfection efficiency of si-NANOG in $H_2O_2$-stimulated HTMCs was measured through RT-PCR and western blotting. **E–H** Protein expression of PI3K, p-Akt, and AKT were measured in HTMCs. Data are shown as individual spots

human ESCs was reduced (K. Chan et al. 2009a, b). Our study also verified that PBX1 activated NANOG transcription via binding to NANOG promoter and NANOG silence suppressed the advantageous effect of PBX1 overexpression on $H_2O_2$-induced cell viability decline and apoptosis in HTMCs. These data showed that NANOG could also act as an important cell survival factor in HTMCs which was regulated by PBX1.

Excessive ROS not only directly results in DNA damage, but also leads to oxidative stress (Nita and Grzybowski 2016). It has been reported that TM cells are sensitive to oxidative stress, presenting as cell loss, apoptosis, disorders of cell cycle, and ECM synthesis (Awai-Kasaoka et al. 2013; Lv et al. 2019). Hence, oxidative stress affected the outflow of AH and further resulted in elevated IOP by impacting the cytoskeleton of TM cells and ECM deposition (Liton et al. 2009; McMonnies 2018; You et al. 2018). Many studies have reported that oxidative stress induced the upregulations of COL1A1, COL4A1, MMPs, vimentin, and fibronectin in TM cells (Rao et al. 2019), which were participated in maintaining and remodeling of TM ECM (You et al. 2018). The high expression of MMP2

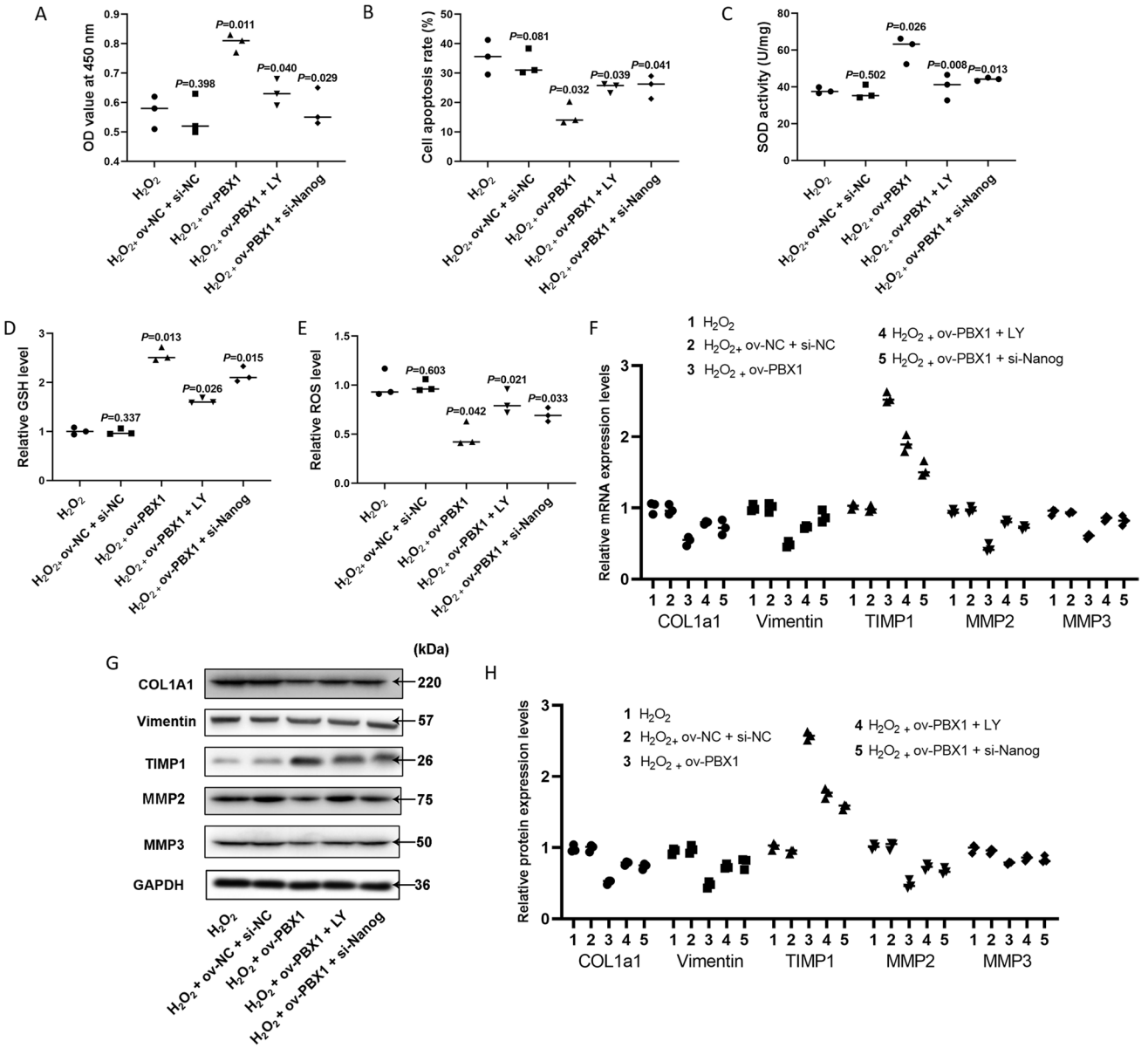


**Fig. 6** Inhibitor of the PI3K or silence of NANOG abolished the protective effect of PBX1 on $H_2O_2$-stimulated (200 μM, 3 h) HTMCs. **A–E** Cell viability (**A**), apoptosis (**B**), SOD activity (**C**), ROS (**D**), and GSH (**E**) levels were measured in $H_2O_2$-stimulated HTMCs. **F–H** Expression levels of ECM metabolism–related genes were analyzed by RT-PCR and western blotting. HTMCs were transfected with ov-PBX1 or ov-PBX1 + si-PBX1 for 24 h, then stimulated with LY294002 (20 μM) for 1 h, and then 200 μM $H_2O_2$ was added into the serum-free medium for 3 h. Approximately post 21 h, cells were harvested for further investigation. Data are shown as individual spots

indicated that tissues were undergoing remodeling (Sahay et al. 2017). TIMP1 is a natural tissue inhibitor of MMPs, and the balance of MMP/TIMP1 affects ECM degradation and AH outflow (O'Callaghan et al. 2017). In this study, we found that PBX1 and NANOG significantly suppressed $H_2O_2$-induced excessive ROS production, promoted the activity of endogenous antioxidative enzyme, SOD, and the level of antioxidant, GSH, also suppressed the expressions of COL1A1, COL4A1, vimentin, fibronectin, MMP2 and MMP3, meanwhile, enhanced TIMP1 expression, while PBX1 inhibition presented the opposite effects. Consistent with our study, a previous study showed that the silence of PBX1 induced ROS production of lung cancer cells (Yao et al. 2020). In addition, growing evidence suggested that PBX1 directly regulated the expression of the antioxidant transcription factor, Nfe2l1, to reduce oxidative stress, mitochondrial dysfunction, and proteasome damage (J. Villaescusa et al. 2016a, b). Consistently, NANOG played a similar antioxidant role in our research. Besides, studies found that NANOG delayed the senescence of stem cells (Andreadis

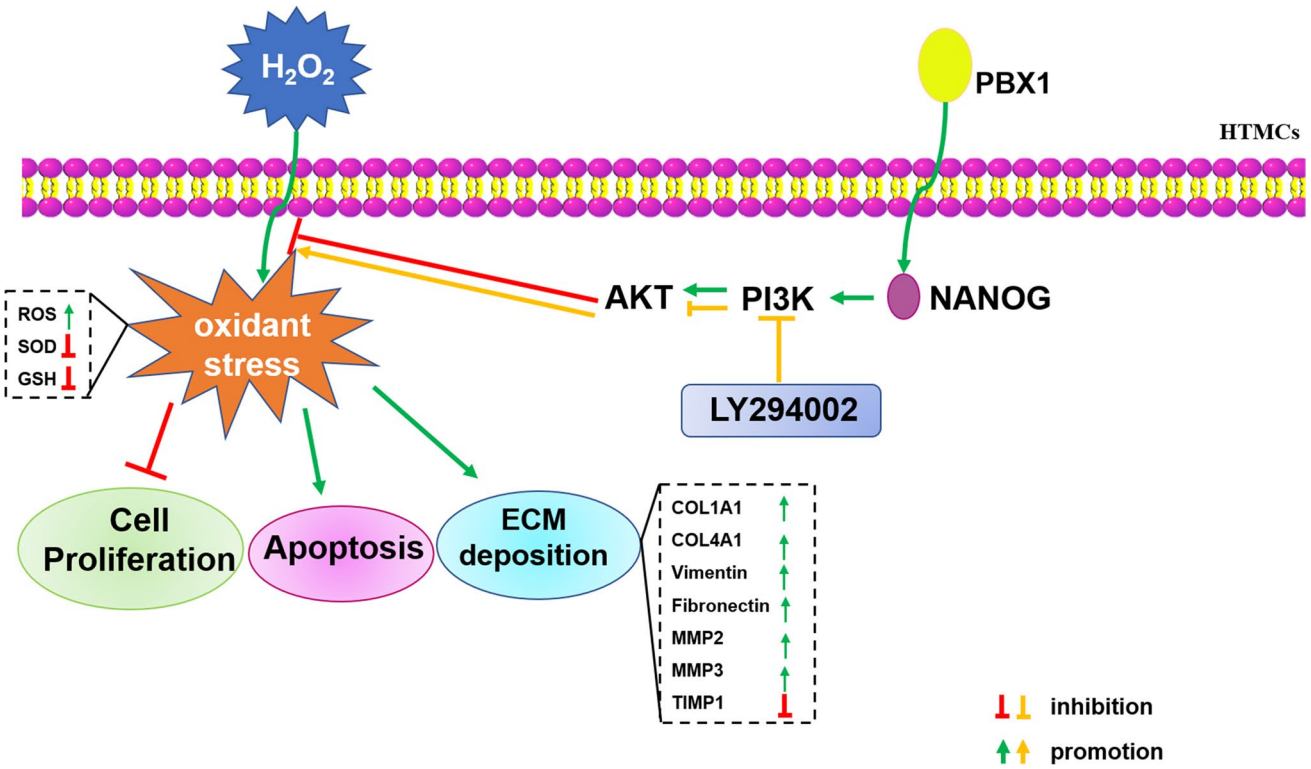


**Fig. 7** Molecular mechanism of PBX1 inhibited $H_2O_2$-induced (200 μM, 3 h) apoptosis, oxidative stress, and ECM deposition in HTMCs. PBX1 promoted the transcription of NANOG through upregulating the promoter activity of NANOG. PBX1 and NANOG depended on the P13K/AKT pathway to reduce oxidative damage which was reflected in suppressing reactive oxygen species (ROS) accumulation and enhancing the productions of superoxide dismutase (SOD) and L-glutathione (GSH). Therefore, PBX1 inhibited cell apoptosis and ECM deposition and promoted cell proliferation. Moreover, LY294002 (an inhibitor of PI3K) partially abolished the effect of PBX1 overexpression in $H_2O_2$-induced HTMCs. The green arrows indicate the effects of $H_2O_2$ on HTMCs, and the yellow symbols indicate the effects of PBX1 in $H_2O_2$-induced HTMCs

et al. 2017), which also supported our conclusion. It was worth noting that we proposed the relationship between PBX1 and ECM deposition and showed the positive role of PBX1 in ECM deposition. Based on these data, our study suggested that PBX1 played a protective role in HTMCs against aggravated oxidative stress and ECM deposition.

P13K/AKT pathway is one of the well-characterized pathways responsible for oxidative stress and regulates cell proliferation, apoptosis, metabolism, and reprogramming. The inhibition of PI3K-AKT pathway decreased the cell viability of $H_2O_2$-treated TM cells (Awai-Kasaoka et al. 2013). Besides, lncRNA-MALAT1 was reported to suppress retinal ganglion cell apoptosis via the activation of PI3K/AKT pathway in a rat model of glaucoma (Li et al. 2017). A previous study indicated that the expression of p-Akt in human retinal pigment epithelial cells was increased after being treated with 200 μM $H_2O_2$ up to 15 min and then decreased slowly (Awai-Kasaoka et al. 2013). Consistently, we found that the PI3K/AKT signaling pathway was activated by $H_2O_2$ at 30 min, and then declined in a time-dependent manner. There was a study that demonstrated that the activation of AKT induced by $H_2O_2$ depended on the epidermal growth factor receptor (EGFR) signaling (Wang et al. 2000). Therefore, the abnormal expression of p-AKT might be due to that $H_2O_2$ treatment led to the phosphorylation of EGFR and inhibited EGFR activation which further prevented the activation of AKT. Additionally, PBX1 promoted the phosphorylation level of AKT and the knockdown of PBX1 decreased the phosphorylation level of AKT in human hair follicle mesenchymal stem cells (Jiang et al. 2019). Our findings also clarified that PBX1 promoted the phosphorylation level of AKT which was reversed by NANOG inhibition. Furthermore, the inactivation of PI3K/AKT signaling or NANOG inhibition suppressed the protective effect of PBX1 on $H_2O_2$-induced HTMCs. It implies that the protective effects of PBX1 on $H_2O_2$-induced HTMCs depend on the activation of PI3K/AKT signaling pathway which was mediated by NANOG.

In summary, our work revealed the protective role of PBX1 in HTMCs under oxidative stress. PBX1 was upregulated in HTMCs under $H_2O_2$ treatment. PBX1 suppressed the cell viability loss, apoptosis, oxidative stress, and ECM

deposition in $H_2O_2$-stimulated HTMCs. Besides, PBX1 activated the PI3K/AKT signaling pathway through promoting the transcriptional activity of NANOG. Our findings highlighted that PBX1 protected HTMCs from $H_2O_2$ injury through activating NANOG-mediated PI3K/AKT signaling pathway. However, the exact role of PBX1/NANOG/P13K/AKT axis in protecting HTMCs from oxidative stress needs to be further verified in animal models *in vivo* in the future.

**Supplementary Information** The online version contains supplementary material available at https://doi.org/10.1007/s12192-022-01304-x.

**Acknowledgements** Not appliable.

**Author contribution** Conceiving the study (LW and SZ), laboratory analyses (LW, YT, YC, SZ), and statistical evaluation (LW, YT, QM), writing the manuscript (LW). All authors read and approved the final paper.

**Data availability** All data are available with the approval of the corresponding author.

## Declarations

**Ethics approval** This is an observational cytology study and does not involve animal or human subjects. No ethical approval is required.

**Conflict of interest** The authors declare no competing interests.

## References

Agarwal P, Agarwal R (2018) Trabecular meshwork ECM remodeling in glaucoma: could RAS be a target? Expert Opin Ther Targets 22:629–638

Ammar DA, Hamweyah KM, Kahook MY (2012) Antioxidants protect trabecular meshwork cells from hydrogen peroxide-induced cell death. Transl Vis Sci Technol 1:4

Andreadis, Stelios T et al (2017) NANOG restores contractility of mesenchymal stem cell-based senescent microtissues. Tissue Engineering Part A

Awai-Kasaoka N, Inoue T, Kameda T et al (2013) Oxidative stress response signaling pathways in trabecular meshwork cells and their effects on cell viability. Mol Vis 19:1332–1340

Bertaud S, Aragno V, Baudouin C et al (2019) Primary open-angle glaucoma. Rev Med Interne 40:445–452

Braunger BM, Fuchshofer R, Tamm ER (2015) The aqueous humor outflow pathways in glaucoma: a unifying concept of disease mechanisms and causative treatment. Eur J Pharm Biopharm 95:173–181

Carreon T, van der Merwe E, Fellman RL et al (2017) Aqueous outflow - a continuum from trabecular meshwork to episcleral veins. Prog Retin Eye Res 57:108–133

Chan K, Zhang J, Chia N et al (2009) KLF4 and PBX1 directly regulate NANOG expression in human embryonic stem cells. Stem Cells (dayton, Ohio) 27:2114–2125

Chan KK, Zhang J, Chia NY et al (2009) KLF4 and PBX1 directly regulate NANOG expression in human embryonic stem cells. Stem Cells 27:2114–2125

Ferraz-de-Souza B, Martin F, Mallet D et al (2009) CBP/p300-interacting transactivator, with Glu/Asp-rich C-terminal domain, 2, and pre-B-cell leukemia transcription factor 1 in human adrenal development and disease. J Clin Endocrinol Metab 94:678–683

Grebbin B, Schulte D (2017) PBX1 as pioneer factor: a case still open. Front Cell Dev Biol 5:9

He S, Stankowska DL, Ellis DZ et al (2018) Targets of neuroprotection in glaucoma. J Ocul Pharmacol Ther 34:85–106

Husain S, Ahmad A, Singh S et al (2017) PI3K/Akt pathway: a role in δ-opioid receptor-mediated RGC neuroprotection. Invest Ophthalmol Vis Sci 58:6489–6499

Izzotti A, Saccà SC, Cartiglia C et al (2003) Oxidative deoxyribonucleic acid damage in the eyes of glaucoma patients. Am J Med 114:638–646

Jiang Y, Liu F, Zou F et al (2019) PBX homeobox 1 enhances hair follicle mesenchymal stem cell proliferation and reprogramming through activation of the AKT/glycogen synthase kinase signaling pathway and suppression of apoptosis. Stem Cell Res Ther 10:268

Jung J-G, Shih I-M, Park JT et al (2016) Ovarian cancer chemoresistance relies on the stem cell reprogramming factor PBX1. Cancer Res 76:6351–6361

Jung JG, Shih IM, Park JT et al (2016) Ovarian cancer chemoresistance relies on the stem cell reprogramming factor PBX1. Cancer Res 76:6351–6361

Kikugawa T, Kinugasa Y, Shiraishi K et al (2006) PLZF regulates Pbx1 transcription and Pbx1–HoxC8 complex leads to androgen-independent prostate cancer proliferation. Prostate 66:1092–1099

Li HB, You QS, Xu LX et al (2017) Long non-coding RNA-MALAT1 mediates retinal ganglion cell apoptosis through the PI3K/Akt signaling pathway in rats with glaucoma. Cell Physiol Biochem 43:2117–2132

Liton PB, Gonzalez P, Epstein DL (2009) The role of proteolytic cellular systems in trabecular meshwork homeostasis. Exp Eye Res 88:724–728

Lv Y, Zhang Z, Xing X et al (2020) lncRNA TGFβ2-AS1 promotes ECM production via TGF-β2 in human trabecular meshwork cells. Biochem Biophys Res Commun 527:881–888

Lv Y, Han X, Yao Q et al (2019) 1α,25-dihydroxyvitamin D3 attenuates oxidative stress-induced damage in human trabecular meshwork cells by inhibiting TGFβ-SMAD3-VDR pathway. Biochem Biophys Res Commun 516:75–81

Magnani L, Ballantyne EB, Zhang X et al (2011) PBX1 genomic pioneer function drives ERα signaling underlying progression in breast cancer. PLoS Genet 7(11):e1002368

McMonnies C (2018) Reactive oxygen species, oxidative stress, glaucoma and hyperbaric oxygen therapy. J Optom 11:3–9

Murphy MJ, Polok BK, Schorderet DF et al (2010) Essential role for Pbx1 in corneal morphogenesis. Invest Ophthalmol vis Sci 51:795–803

Nita M, Grzybowski A (2016) The role of the reactive oxygen species and oxidative stress in the pathomechanism of the age-related ocular diseases and other pathologies of the anterior and posterior eye segments in adults. Oxid Med Cell Longev 2016:3164734

O'Callaghan J, Cassidy PS, Humphries P (2017) Open-angle glaucoma: therapeutically targeting the extracellular matrix of the conventional outflow pathway. Expert Opin Ther Targets 21:1037–1050

Okada S, Irié T, Tanaka J et al (2015) Potential role of hematopoietic pre-B-cell leukemia transcription factor-interacting protein in oral carcinogenesis. J Oral Pathol Med 44:115–125

Pinazo-Duran M, Shoaie-Nia K, Zanon-Moreno V et al (2018) Strategies to reduce oxidative stress in glaucoma patients. Curr Neuropharmacol 16:903–918

Rao VR, Lautz JD, Kaja S et al (2019) Mitochondrial-targeted antioxidants attenuate TGF-β2 signaling in human trabecular meshwork cells. Invest Ophthalmol vis Sci 60:3613–3624

Saccà SC, Gandolfi S, Bagnis A et al (2016) From DNA damage to functional changes of the trabecular meshwork in aging and glaucoma. Ageing Res Rev 29:26–41

Sahay P, Rao A, Padhy D et al (2017) Functional activity of matrix metalloproteinases 2 and 9 in tears of patients with glaucoma. Invest Ophthalmol Vis Sci 58:Bio106-bio113

Schnabel CA, Selleri L, Cleary ML (2003) Pbx1 is essential for adrenal development and urogenital differentiation. Genesis 37:123–130

Shiraishi K, Yamasaki K, Nanba D et al (2007) Pre-B-cell leukemia transcription factor 1 is a major target of promyelocytic leukemia zinc-finger-mediated melanoma cell growth suppression. Oncogene 26:339–348

Teoh PH, Shu-Chien AC, Chan WK (2010) Pbx1 is essential for growth of zebrafish swim bladder. Dev Dyn:Off Publ Am Assoc Anatomists 239:865–874

Villaescusa J, Li B, Toledo E et al (2016a) A PBX1 transcriptional network controls dopaminergic neuron development and is impaired in Parkinson's disease. EMBO J 35:1963–1978

Villaescusa JC, Li B, Toledo EM et al (2016b) A PBX1 transcriptional network controls dopaminergic neuron development and is impaired in Parkinson's disease. Embo J 35:1963-1978

Wang B, Liu F, Liu Z et al (2020) Internalization of the TAT-PBX1 fusion protein significantly enhances the proliferation of human hair follicle-derived mesenchymal stem cells and delays their senescence. Biotechnol Lett 42:1877–1885

Wang J, Qu D, An J et al (2017) Integrated microarray analysis provided novel insights to the pathogenesis of glaucoma. Mol Med Rep 16:8735–8746

Wang M, Hu R, Wang Y et al (2019) Atractylenolide III attenuates muscle wasting in chronic kidney disease via the oxidative stress-mediated PI3K/AKT/mTOR pathway. Oxid Med Cell Longev 2019:1875471

Wang X, McCullough K, Franke T et al (2000) Epidermal growth factor receptor-dependent Akt activation by oxidative stress enhances cell survival. J Biol Chem 275:14624–14631

Wu R, Xue P, Wan Y et al (2018) LncRNA-uc.40 silence promotes P19 embryonic cells differentiation to cardiomyocyte via the PBX1 gene. In Vitro Cell Dev Biol Anim 54:600–609

Yao X, Peng H, Wu J (2020) Silencing PBX1 expression induces apoptosis and ROS production of lung cancer cells. Zhonghua Zhong Liu Za Zhi [Chin J Oncol] 42:843–848

You ZP, Zhang YZ, Zhang YL et al (2018) Homocysteine induces oxidative stress to damage trabecular meshwork cells. Exp Ther Med 15:4379–4385

Zhuang Y, Wu H, Wang X et al (2019) Resveratrol attenuates oxidative stress-induced intestinal barrier injury through PI3K/Akt-mediated Nrf2 signaling pathway. Oxid Med Cell Longev 2019:7591840